NACA RM L56B20

NACA

RESEARCH MEMORANDUM

FREE-FLIGHT INVESTIGATION OF THE CONTROL EFFECTIVENESS OF A DIFFERENTIALLY DEFLECTED HORIZONTAL TAIL AT MACH NUMBERS FROM 0.8 TO 1.6

By Jesse L. Mitchell and A. James Vitale

Langley Aeronautical Laboratory
Langley Field, Va.

NATIONAL ADVISORY COMMITTEE
FOR AERONAUTICS

WASHINGTON

April 26, 1956
Declassified February 26, 1958

NACA RM L56B20

NATIONAL ADVISORY COMMITTEE FOR AERONAUTICS

RESEARCH MEMORANDUM

FREE-FLIGHT INVESTIGATION OF THE CONTROL EFFECTIVENESS OF A DIFFERENTIALLY DEFLECTED HORIZONTAL TAIL AT MACH NUMBERS FROM 0.8 TO 1.6

By Jesse L. Mitchell and A. James Vitale

SUMMARY

The Pilotless Aircraft Research Division of the Langley Aeronautical Laboratory has made a free-flight investigation of the control effectiveness of a differentially deflected horizontal tail. The results of the investigation were compared with and found to be in general agreement with estimates derived from other free-flight tests, wind-tunnel tests, and theory. These results indicate that the rolling moment of the differentially deflected horizontal tail has relatively small variation with Mach number over the range of the test and that the yawing moment, in a direction usually referred to as favorable, is about two to three times as great as the rolling moment and has a comparatively large variation with Mach number. The yawing moment is partly the result of pressures induced on the vertical tail-fuselage (herein called induced yawing moment) and partly the result of the negative dihedral of the present horizontal tail. The results of calculations based on the present test results, theory, and wind-tunnel test indicate that about one-half the total yawing moment at subsonic speeds is induced yawing moment. Calculations based on the present test results and theory indicate that this induced yawing moment decreases rapidly in both absolute magnitude and in relative proportion to the total moment with increasing Mach number at supersonic speeds.

INTRODUCTION

The use of all-movable horizontal tails as a lateral-control device has been considered in several recent investigations. Some control-effectiveness data for an unswept horizontal tail at a Mach number of 0.13 are given in reference 1 and at Mach numbers from 0.25 to 0.95 in reference 2. Control-effectiveness data for a 45° sweptback tail at Mach numbers from 0.8 to 1.05 are given in reference 3. The overall rolling

effectiveness, in terms of the wing-tip helix angle, of a configuration having a 45° sweptback tail and a notched delta wing at Mach numbers from 0.6 to 1.5 is presented in reference 4 and includes some effects of aeroelasticity. A brief summary of the use of the horizontal tail for roll control is given in reference 5.

As part of a general research investigation of the lateral stability characteristics of airplane configurations conducted by the Pilotless Aircraft Research Division, an airplane configuration with a 45° sweptback wing and horizontal tail, and a 60° sweptback vertical tail was flown with the horizontal tail pulsed differentially during the flight. The purpose of the present report is to present the experimental results obtained in the Mach number range 0.8 to 1.6 for the control effectiveness of the horizontal tail. The Reynolds number range based on horizontal-tail mean aerodynamic chord was 1.5×10^6 to 5.1×10^6 and the range of angle of attack and angle of sideslip was 0° to 4°. Results are presented for the rolling-moment effectiveness, the yawing-moment effectiveness, and the overall effectiveness in terms of the trim values of wing-tip helix angle, angle of sideslip, and angle of attack of the configuration. These experimental data are compared with other results obtained from references 3, 4, and 6. In addition, the effects of aeroelasticity of the horizontal tail on the measured effectiveness have been estimated and the results are included in the present report.

SYMBOLS

C_l	rolling-moment coefficient, $\frac{\text{Rolling moment}}{qSb}$
C_n	yawing-moment coefficient, $\frac{\text{Yawing moment}}{qSb}$
C_Y	side-force coefficient, $\frac{\text{Side force}}{qS}$
q	dynamic pressure, lb/sq ft
S	total wing area, sq ft
b	wing span, ft
α	angle of attack, deg
β	angle of sideslip, deg

i_t	horizontal-tail incidence (parallel to free stream, positive for trailing edge down, and measured in plane parallel to plane of symmetry), deg
i_{td}	differential-tail incidence (i_t of left tail - i_t of right tail), deg
p	rolling velocity, radians/sec
V	velocity, ft/sec
θ/L	structural influence coefficient, local streamwise twist angle produced by a unit concentrated load, radians/lb
y	lateral distance from fuselage center line, ft
b_t	horizontal-tail span, ft
S_t	horizontal-tail area, ft^2
Γ	dihedral angle, deg
C_{l_p}	damping-in-roll derivative, $\frac{\partial C_l}{\frac{\partial pb}{2V}}$, 1/radian
c	chord, ft
$\bar{c}$	wing mean aerodynamic chord, ft
$\bar{c}_t$	horizontal-tail mean aerodynamic chord, ft
A	aspect ratio
$\Lambda_{c/4}$	sweepback of quarter-chord line, deg
λ	taper ratio
$\frac{b_e}{b_t}$	ratio of exposed span to total span for horizontal tail
R	Reynolds number
M	Mach number

$\frac{p}{p_o}$ ratio of atmospheric pressure, p, to standard sea-level pressure, p_o (where p_o = 2,116 lb/sq ft)

$\frac{\Delta i_{te}}{i_t}$ ratio of incremental tail-incidence change due to aeroelasticity to incidence of tail root chord

K factor for converting measured control-effectiveness data to rigid values

l_t tail length

Subscripts:

i induced effect

Γ dihedral effect

MODEL AND TESTS

Model

The present configuration is the same as that of reference 7 as regards both geometry and construction. The general physical characteristics of the model are shown in figure 1, table I, figure 2, and the following table:

Weight, lb	155
Center of gravity, percent mean aerodynamic chord	26.1
Moments of inertia:	
Pitch, slug-ft^2	9.06
Yaw, slug-ft^2	9.92
Roll, slug-ft^2	1.11

The measured structural influence coefficients of the solid dural horizontal tail are presented in figure 3. Similar data for the solid steel wing may be found in reference 7.

Flight Test

The flight test was conducted at the Pilotless Aircraft Research Station at Wallops Island, Va. The model with its solid-propellant rocket boost system was launched at an angle of 70°. The model separated from the booster at a peak Mach number of 1.7, and the data were obtained

throughout the coasting period of the model flight. During the coasting flight, the horizontal tails were deflected differentially by means of an electrohydraulic system.

Data telemetered from the model included the following which were necessary to obtain the results presented: rate of roll, right and left horizontal-tail incidence, transverse accelerations near the center of gravity and at a point in the nose, angles of attack and sideslip, and total pressure.

Data obtained from tracking radar, Doppler radar, and radiosonde were model flight path, velocity, and atmospheric test conditions.

The static-pressure ratio and Reynolds number of the test are given in figures 4 and 5 as a function of Mach number.

ANALYSIS

Experimental Results

The basic measurements were converted to time histories of the various quantities needed for the present report (see fig. 6) by methods discussed extensively in previous rocket-model reports. (For example, see ref. 8.)

An examination of figure 6 indicates the procedures followed in obtaining the results presented in the present report. The incremental values of rolling moment ΔC_l and yawing moment ΔC_n which occurred when the horizontal tail was deflected abruptly from a differential-tail incidence $i_{t_d} = 0^\circ$ to $i_{t_d} = 8^\circ$ (or from $i_{t_d} = 8^\circ$ to $i_{t_d} = 0^\circ$) were each divided by the incremental change in differential-tail deflection $\Delta i_{t_d} = 8^\circ$ (or $\Delta i_{t_d} = -8^\circ$). These results were considered to be the total rolling effectiveness $\Delta C_l/\Delta i_{t_d}$ and the total yawing effectiveness $\Delta C_n/\Delta i_{t_d}$.

Final or trim values of $pb/2V$, β, and α were determined by drawing mean lines through their oscillatory responses to the abrupt control deflection.

Comparative Data

The experimental results of references 3, 4, and 6 were used to estimate rolling-moment effectiveness $\Delta C_l/\Delta i_{t_d}$ and yawing-moment effectiveness $\Delta C_n/\Delta i_{t_d}$ to compare with the present test results.

Table II presents some of the pertinent physical characteristics of the present control and the control of references 3 and 4.

Rolling-moment effectiveness $\Delta C_l/\Delta i_{td}$ was estimated directly from the data of reference 3 as follows:

$$\frac{\Delta C_l}{\Delta i_{td}} = \left(\frac{\Delta C_l}{\Delta i_{td}} \frac{Sb}{S_t b_t}\right)_{ref} \left(\frac{S_t b_t}{Sb} \cos \Gamma\right)_{test}$$

where a term $\cos \Gamma$, the cosine of the dihedral angle of the present horizontal tail, is included in this equation and all subsequent equations to account for the fact that the incidence is measured in planes parallel to the plane of symmetry. An indirect estimate of $\Delta C_l/\Delta i_{td}$ was made by utilizing the total rolling effectiveness $\frac{pb/2V}{\Delta i_{td}}$ from reference 4 for the aluminum wing configuration in conjunction with the damping in roll for this configuration estimated from the data of reference 6 as follows:

$$\frac{\Delta C_l}{\Delta i_{td}} = -1.08\left(\frac{pb/2V}{\Delta i_{td}} \frac{Sb}{S_t b_t} C_{l_p}\right)_{ref} \left(\frac{S_t b_t}{Sb} \cos \Gamma\right)_{test}$$

where the factor 1.08, to account for the difference in exposed span to total span ratio between the reference control and the present control, was obtained from reference 9.

The induced yawing moment $\left(\Delta C_n/\Delta i_{td}\right)_i$ was estimated from the induced-side-force data of reference 3 as follows:

$$\left(\frac{\Delta C_n}{\Delta i_{td}}\right)_i = -\left(\frac{\Delta C_Y}{\Delta i_t} \frac{S}{S_t}\right)_{ref} \left(\frac{S_t l_t}{Sb} \cos \Gamma\right)_{test}$$

The yawing moment arising from the dihedral was taken to be

$$\left(\frac{\Delta C_n}{\Delta i_{td}}\right)_\Gamma = \left(\frac{C_n}{C_l}\right)_\Gamma \frac{\Delta C_l}{\Delta i_{td}}$$

where $\left(\frac{C_n}{C_l}\right)_\Gamma$, the ratio of yawing moment arising from the dihedral of

the horizontal tail to the total rolling moment, was determined from some calculated span loadings discussed subsequently in this section; $\Delta C_l/\Delta i_{td}$ is the estimate of rolling moment for the present configuration from the data of reference 3.

Theoretical Calculations

The rolling moment of the horizontal tail, neglecting induced effects on the fuselage and vertical tail, was estimated from loading calculations. Rigid tail loadings were estimated at subsonic speeds by use of reference 10. At supersonic speeds (Mach numbers above which the trailing edge was supersonic), rigid tail loadings were estimated from references 11, 12, and 13 to be those of a half-wing equal to the exposed portion of the horizontal tail. The rigid tail loadings were used in conjunction with the data from figures 3 and 4 to obtain span loadings corrected for aeroelasticity. Values of the rolling-moment effectiveness $\Delta C_l/\Delta i_{td}$ were then estimated from these loadings and the results were compared with the experimental data.

The ratio of yawing moment arising from the dihedral of the horizontal tail to the total rolling moment $\left(\frac{C_n}{C_l}\right)_\Gamma$ was also calculated from the span loadings corrected for aeroelasticity.

The estimated aeroelastic properties of the control surface for the present test conditions are summarized in figure 7. The calculated twist distribution due to aeroelasticity for three Mach numbers is given in figure 7(a), and the ratio of rigid to elastic control effectiveness is presented as a function of Mach number in figure 7(b).

ACCURACY

On the basis of instrument accuracy and experience, the average accuracy of the experimental results presented herein is believed to be within the following limits:

$\frac{\Delta C_l}{\Delta i_{td}}$	± 0.00006
$\frac{\Delta C_n}{\Delta i_{td}}$	± 0.0002
$\frac{pb}{2V}$	± 0.001
β, deg	$\pm\frac{1}{2}$
α, deg	$\pm\frac{1}{2}$

RESULTS AND DISCUSSION

General

Figures 8, 9, and 10 show the variation of trim angle of attack α_{trim}, trim angle of sideslip β_{trim}, and trim wing-tip helix angle $(pb/2V)_{trim}$, respectively, with Mach number for the model with differential-tail incidence i_{td} of 0° and 8°. The measured control-effectiveness parameters $\Delta C_l/\Delta i_{td}$ and $\Delta C_n/\Delta i_{td}$ plotted as a function of Mach number are shown in figure 11.

The data points for α_{trim}, β_{trim}, and $(pb/2V)_{trim}$ below a Mach number of 0.95 are flagged and should be considered as only an indication of the test conditions. The reasons for this are twofold. First, the character of the response to the control deflection below $M = 0.95$ was such that a final or trim value could not be determined accurately before the control pulsed to the next position; second, there is the possibility that the usual steady-state trim does not exist since calculations indicate that a divergent mode of motion occurs at the differential-tail setting of 8° as the rate of roll approaches the natural frequency of the dutch-roll mode of motion.

The data points for $\Delta C_l/\Delta i_{td}$ and $\Delta C_n/\Delta i_{td}$ of figure 11 are identified as to the angle-of-attack and angle-of-sideslip conditions. The unflagged points were obtained at the angle of attack, angle of sideslip, and roll rate given by the trim curves for $i_{td} = 0^\circ$ in figures 8, 9, and 10 ($\alpha = \beta \approx 0$). The flagged points were obtained for the conditions indicated by the trim curves for $i_{td} = 8^\circ$. At the highest Mach numbers there is some apparent consistency in the results with respect to trim conditions. In view of the estimated accuracy of the data, however, no further distinction will be made regarding possible effects due to angle of attack, angle of sideslip, or roll rate, and subsequent discussion of effectiveness will be confined to the average curve faired through all the data points.

Rolling Moment

The average measured rolling effectiveness from figure 11 is shown again in figure 12, along with estimates made from other data, references 3, 4, and 6, and results obtained from a theoretical calculation. (See section entitled "Analysis" regarding the details of both experimental and theoretical comparisons.) All the results indicate the same general level of effectiveness and only small or no variation of this effectiveness with Mach number; however, the present test results are

consistently lower than any of the other estimations. The accuracy of the various estimates is not good enough to warrant a conclusion regarding these consistently lower values, but the differences in taper ratio and gap between the present control and those of references 3 and 4 should be noted in table II. As indicated on the figure, the results shown for the present test and those calculated theoretically for the present test include the effects of aeroelasticity since the comparative data results, as far as can be ascertained from references 3 and 4, have not been corrected for aeroelasticity. The comparisons should be reasonably valid on this basis since all the tails were of solid aluminum construction and the test conditions were roughly the same. The rigid control effectiveness may be estimated by multiplying the measured values of control effectiveness (fig. 11 or fig. 12) by the calculated aeroelastic correction factor of figure 7.

Yawing Moment

The value of yawing-moment effectiveness $\Delta C_n/\Delta i_{td}$ (see fig. 11) is the order of two to three times as great as the rolling-moment effectiveness and shows a relatively larger variation with Mach number. This yawing moment is of the same sign as the rolling moment (sometimes referred to as favorable yaw) and comes primarily from two sources. First, the fact that the horizontal tail has negative dihedral gives rise to a component of side force on the horizontal tail and thus to what will be referred to herein as the yawing moment due to dihedral. Second, a side force is induced on the vertical tail and fuselage because of the pressure fields generated by the differential incidence, and this results in what will be referred to as an induced yawing moment. Both of these yawing moments are in the same direction for the present test and, thus, have additive effects on the total yawing moment.

The data of reference 3 indicate that the induced side force has very little effect on the rolling moment of the horizontal tail. In addition, calculations referred to in the analysis section indicated that the ratio of yawing moment due to dihedral to the total rolling moment $\left(\frac{C_n}{C_l}\right)_\Gamma$ varied only from 1.43 to 1.56 for the Mach number range of the test. On this basis, an estimate of induced yawing moment was made by subtracting an estimated dihedral effect from the total yawing moment as follows:

$$\left(\frac{\Delta C_n}{\Delta i_{td}}\right)_i = \left(\frac{\Delta C_n}{\Delta i_{td}}\right)_{test} - \left(\frac{C_n}{C_l}\right)_\Gamma \left(\frac{\Delta C_l}{\Delta i_{td}}\right)_{test}$$

The breakdown of the yawing-moment effectiveness as thus deduced from the rocket-model data is presented in figure 13. Also shown is another estimate of the yawing moments made by use of the data of reference 3. (See section entitled "Analysis.") The induced effect, on the basis of both the estimate from the present test and the estimate from the data of reference 3, is about one-half the total in the Mach number range from 0.8 to 1.05. Above this Mach number, on the basis of the rocket-model estimate, the induced effect decreases rapidly with increasing Mach number.

Overall Rolling Effectiveness

The measured rolling effectiveness in terms of $\frac{\Delta(pb/2V)}{\Delta i_{td}}$ as a function of Mach number is shown in figure 14. These results include the effect of the yawing moment of the tail and, hence, rolling moments due to angle of sideslip and rate of yaw. An estimate of the rolling effectiveness $\frac{\Delta(pb/2V)}{\Delta i_{td}}$ for an assumed case in which the deflection of the horizontal tail contributes no yawing moment was made by dividing the rolling-moment results from either figure 11 or figure 12 by the damping in roll as obtained from some unpublished results of the present test. The results of this estimate are also shown in figure 14 and indicate that, for the present configuration and test conditions (including aeroelastic effects), a level of total effectiveness $\frac{\Delta(pb/2V)}{\Delta i_{td}}$ for the assumed case of zero yawing-moment input, of about 0.0013 in the Mach number range 0.9 to 1.6.

CONCLUDING REMARKS

The results of a free-flight investigation at Mach numbers from 0.8 to 1.6 of the rolling effectiveness of a differentially deflected horizontal tail and the comparison of these results with other free-flight tests, wind-tunnel tests, and theory indicate the following concluding remarks.

The results of the present investigation are in general agreement with the comparable results. These results indicate that the rolling moment of the differentially deflected horizontal tail has relatively small variation with Mach number over the range of the test and that the yawing moment, in a direction usually referred to as favorable, is about two to three times as great as the rolling moment and has a comparatively large variation with Mach number. The yawing moment is

partly the result of pressures induced on the vertical tail and fuselage (herein called induced yawing moment) and partly the result of the negative dihedral of the present horizontal tail. The results of calculations based on the present test results, theory, and wind-tunnel tests indicate that about one-half the total yawing moment at subsonic speeds is induced yawing moment. Calculations based on the present test results and theory indicate that this induced yawing moment decreases rapidly in both absolute magnitude and in relative proportion to the total moment with increasing Mach number at supersonic speeds.

Langley Aeronautical Laboratory,
National Advisory Committee for Aeronautics,
Langley Field, Va., February 7, 1956.

REFERENCES

1. Koenig, David G.: Tests in the Ames 40- by 80-Foot Wind Tunnel of an Airplane Configuration With an Aspect Ratio 3 Triangular Wing and an All-Movable Horizontal Tail - Longitudinal and Lateral Characteristics. NACA RM A52L15, 1953.

2. Savage, Howard F., and Tinling, Bruce E.: The Static Lateral and Directional Subsonic Aerodynamic Characteristics of an Airplane Model Having a Triangular Wing of Aspect Ratio 3. NACA RM A55B11, 1955.

3. Critzos, Chris C.: Lateral-Control Investigation at Transonic Speeds of Differentially Deflected Horizontal-Tail Surfaces for a Configuration Having a 6-Percent-Thick 45° Sweptback Wing. NACA RM L55I26, 1955.

4. English, Roland D.: Free-Flight Investigation, Including Some Effects of Wing Aeroelasticity, of the Rolling Effectiveness of an All-Movable Horizontal Tail With Differential Incidence at Mach Numbers From 0.6 to 1.5. NACA RM L54K30, 1955.

5. Campbell, John P.: The Use of the Horizontal Tail For Roll Control. NACA RM L55L16a, 1956.

6. Bland, William M., Jr.: Effect of Wing Flexibility on the Damping in Roll of a Notched Delta Wing-Body Combination Between Mach Numbers 0.6 and Approximately 2.2 As Determined With Rocket-Propelled Models. NACA RM L54E04, 1954.

7. McFall, John C., Jr.: Longitudinal Stability Investigation For a Mach Number Range of 0.8 to 1.7 of an Airplane Configuration With a 45° Swept Wing and a Low Horizontal Tail. NACA RM L55L09, 1956.

8. Mitchell, Jesse L., and Peck, Robert F.: Investigation of The Lateral Stability Characteristics of the Douglas X-3 Configuration at Mach Numbers From 0.6 to 1.1 by Means of a Rocket-Propelled Model. NACA RM L54L20, 1955.

9. Strass, H. Kurt, Stephens, Emily W., Fields, Edison M., and Schult, Eugene D.: Collection And Summary of Flap-Type-Aileron Rolling-Effectiveness Data at Zero Lift As Determined by Rocket-Powered Model Tests at Mach Numbers Between 0.6 and 1.6. NACA RM L55F14, 1955.

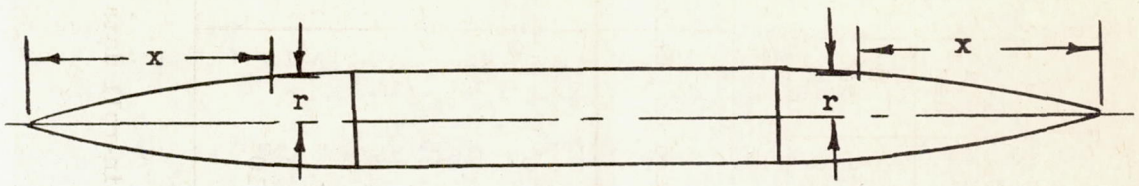
10. DeYoung, John: Theoretical Antisymmetric Span Loading for Wings of Arbitrary Plan Form at Subsonic Speeds. NACA Rep. 1056, 1951. (Supersedes NACA TN 2140.)

11. Heaslet, Max. A., Lomax, Harvard, and Jones, Arthur L.: Volterra's Solution of the Wave Equation As Applied to Three-Dimensional Supersonic Airfoil Problems. NACA Rep. 889, 1947. (Supersedes NACA TN 1412.)

12. Goodman, Theodore R.: The Lift Distribution on Conical and Nonconical Flow Regions of Thin Finite Wings in a Supersonic Stream. Jour. Aero. Sci., vol. 16, no. 6, June 1949, pp. 365-374.

13. Margolis, Kenneth: Theoretical Calculations of the Pressures, Forces, and Moments Due to Various Lateral Motions Acting on Thin Isolated Vertical Tails With Supersonic Leading and Trailing Edges. NACA TN 3373, 1955.

TABLE I.- FUSELAGE NOSE AND TAIL ORDINATES

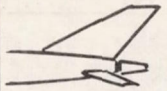
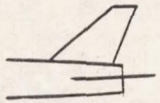
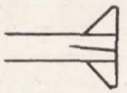


x, in.	r, in.
0	0.168
.060	.182
.122	.210
.245	.224
.480	.294
.735	.350
1.225	.462
2.000	.639
2.450	.735
4.800	1.245
7.350	1.721
8.000	1.849
9.800	2.155
12.250	2.505
13.125	2.608
14.375	2.747
14.700	2.785
17.150	3.010
19.600	3.220
22.050	3.385
24.500	3.500

TABLE II.- COMPARISON OF PRESENT HORIZONTAL TAIL

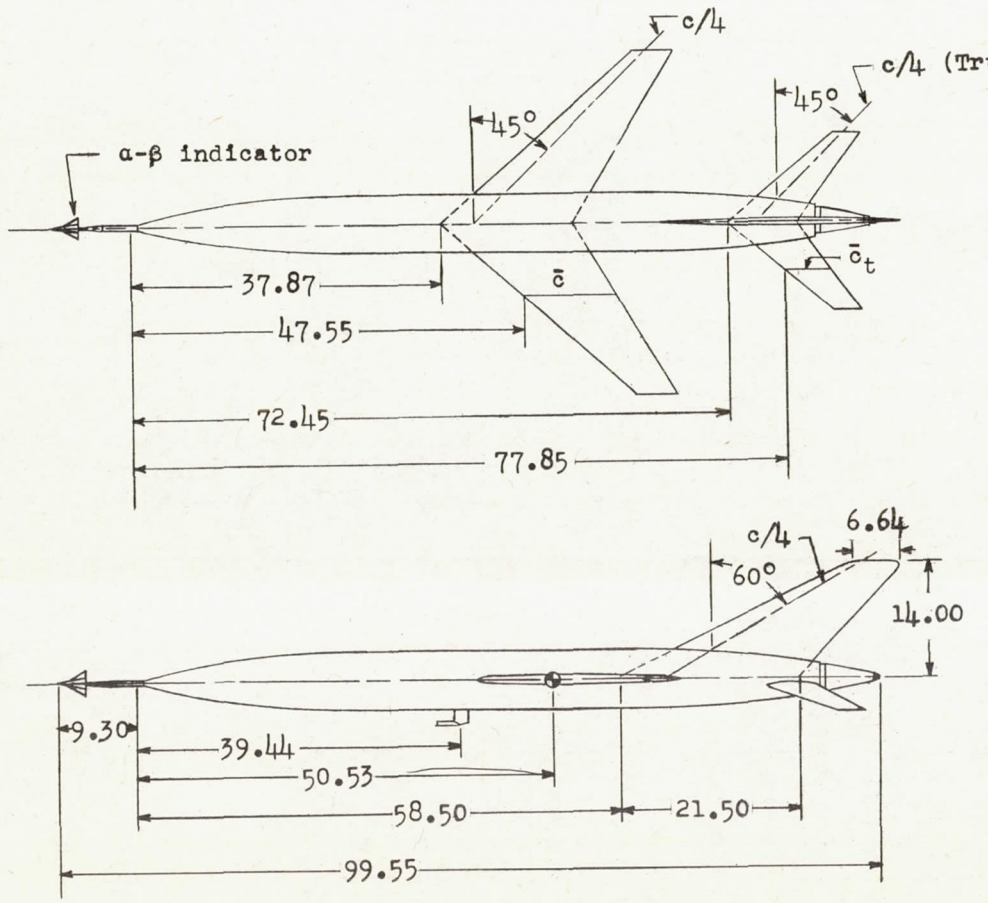
WITH OTHERS TESTED

	A	$\Lambda_{c/4}$, deg	λ	Airfoil	Γ, deg	$\frac{b_e}{b_t}$	Δi_{td}, deg
Present test	[a]4	[a]45	0.4	NACA [a]65A006	-20	0.78	8
Reference 3	4	45	.6	NACA 65A006	0	.78	-20
Reference 4[b]	4	45	.6	NACA 65A006	0	.69	14

Gap	Vertical tail and afterbody	Construction	Reynolds number range based on $\bar{c}_t$	Mach number range
About 1 percent of semispan		Solid aluminum alloy	1.5×10^6 to 5.1×10^6	0.8 to 1.6
Sealed		Solid aluminum alloy	2.3×10^6 to 2.7×10^6	0.8 to 1.05
Sealed		Solid aluminum alloy	1.3×10^6 to 3.1×10^6	0.6 to 1.4

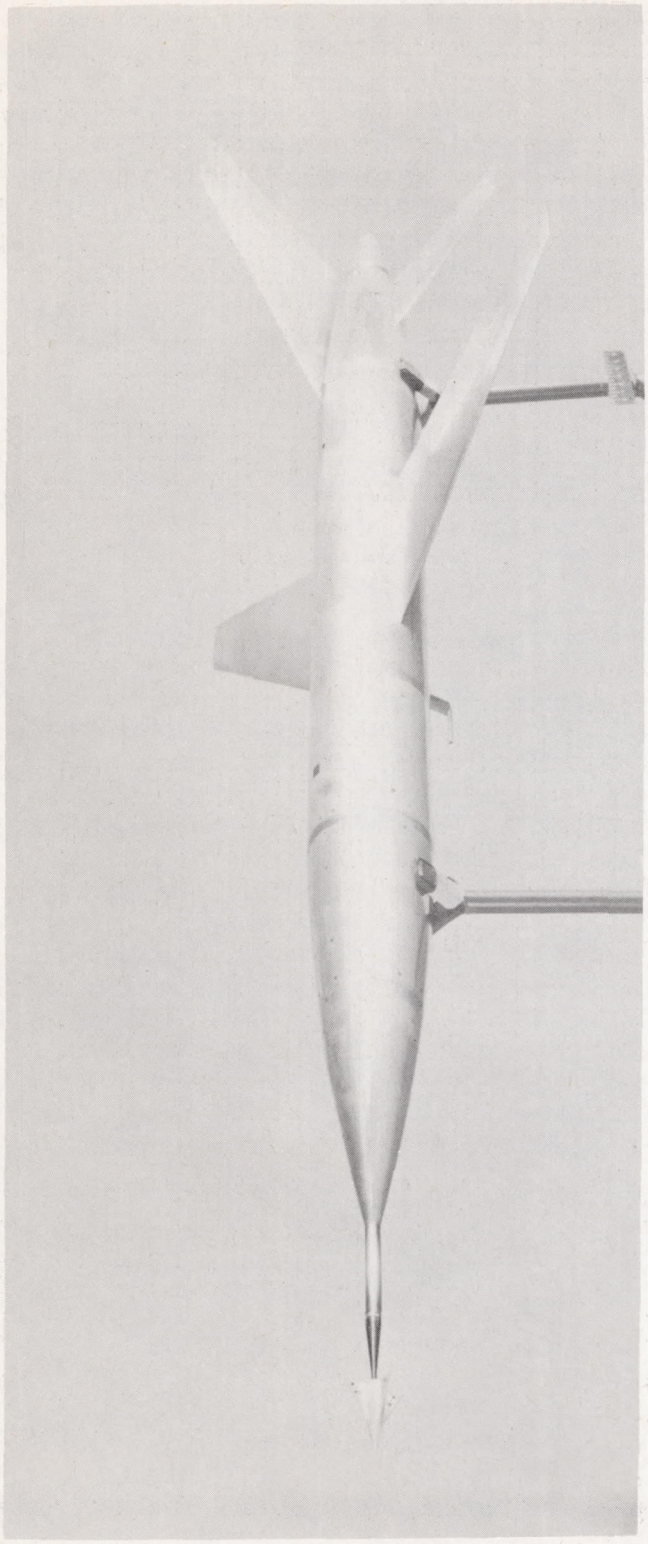
[a]True view; that is, with zero dihedral.

[b]Data on total effectiveness pb/2V. Results combined with damping-in-roll data of reference 6 to obtain rolling effectiveness $\Delta C_l/\Delta i_{td}$.



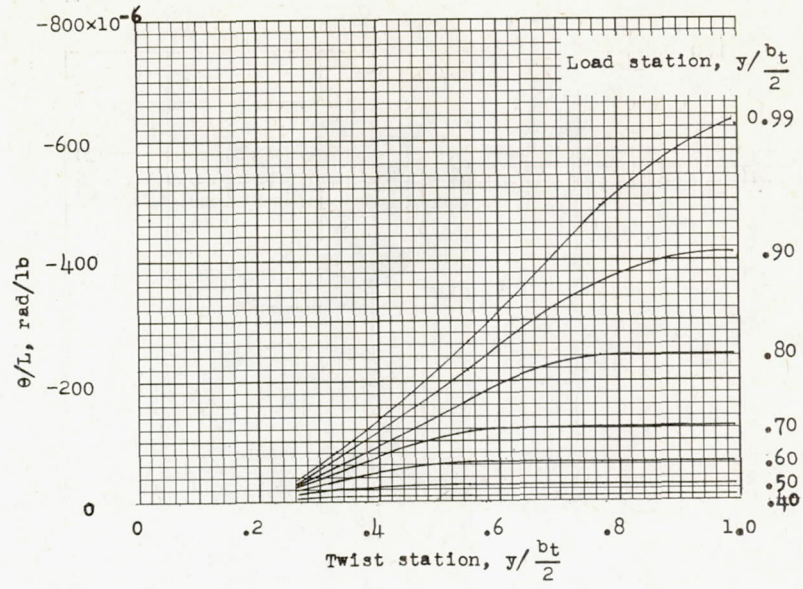
Horizontal tail		
Aspect ratio	4.00	
Taper ratio	0.40	
Area (total), sq ft	0.905	
M.A.C., ft	0.504	
Hinge line, chord	0.42	
Dihedral, deg	-20.00	
Airfoil section	NACA	65A006
Vertical tail		
Area (total), sq ft	1.37	
Airfoil section	NACA	65A003
Wing		
Aspect ratio	4.00	
Taper ratio	0.30	
Area (total), sq ft	3.00	
M.A.C., ft	0.95	
Airfoil section	NACA	65A006

Figure 1.- General arrangement of model. All dimensions are in inches unless otherwise indicated.

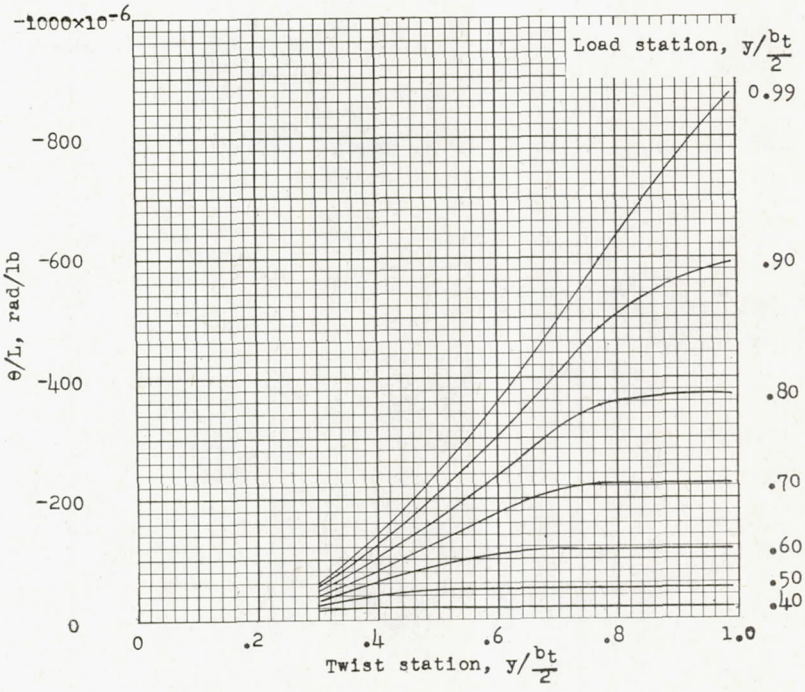


L-86914

Figure 2.- Photograph of model.



(a) 0.25c loading.



(b) 0.50c loading.

Figure 3.- Structural influence coefficients for horizontal tail.

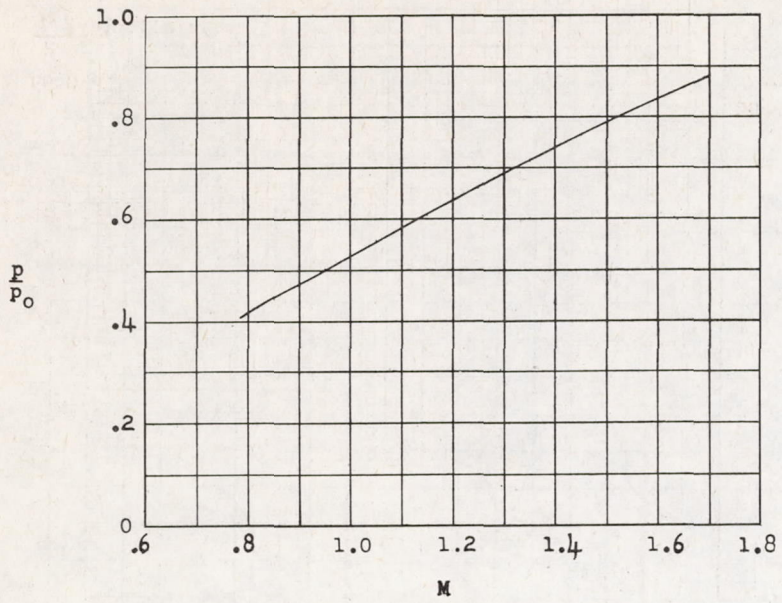


Figure 4.- Static-pressure ratio.

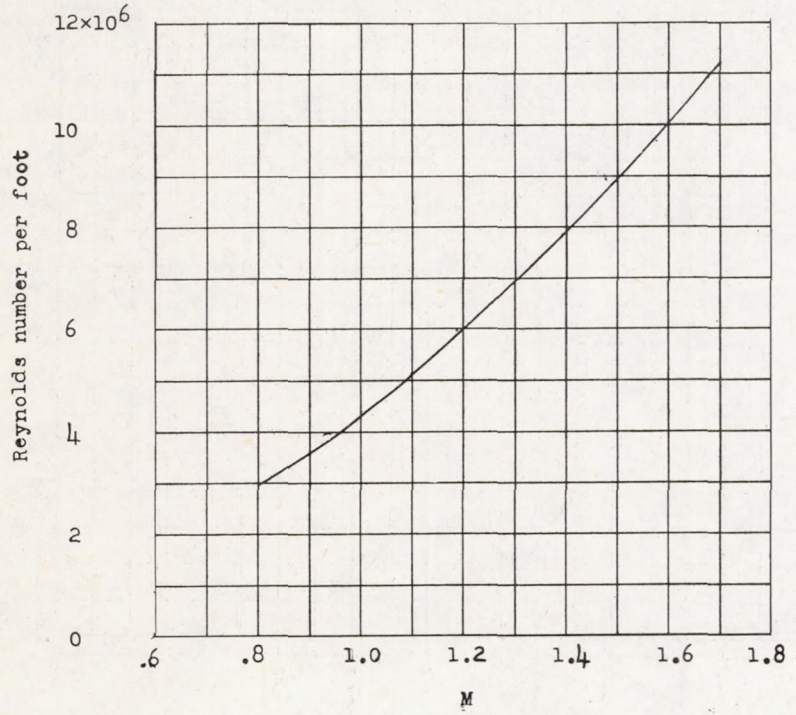


Figure 5.- Reynolds number of test.

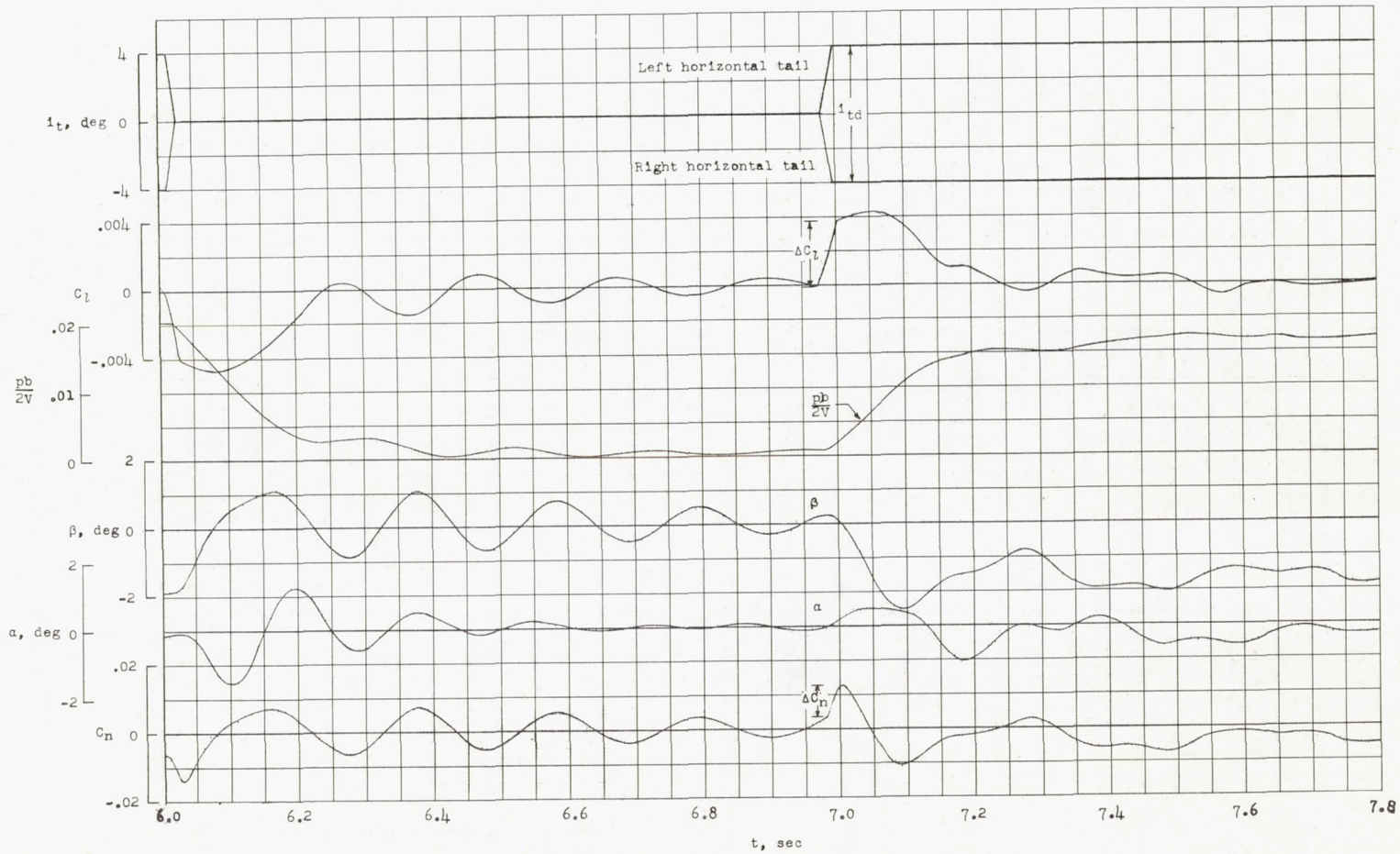
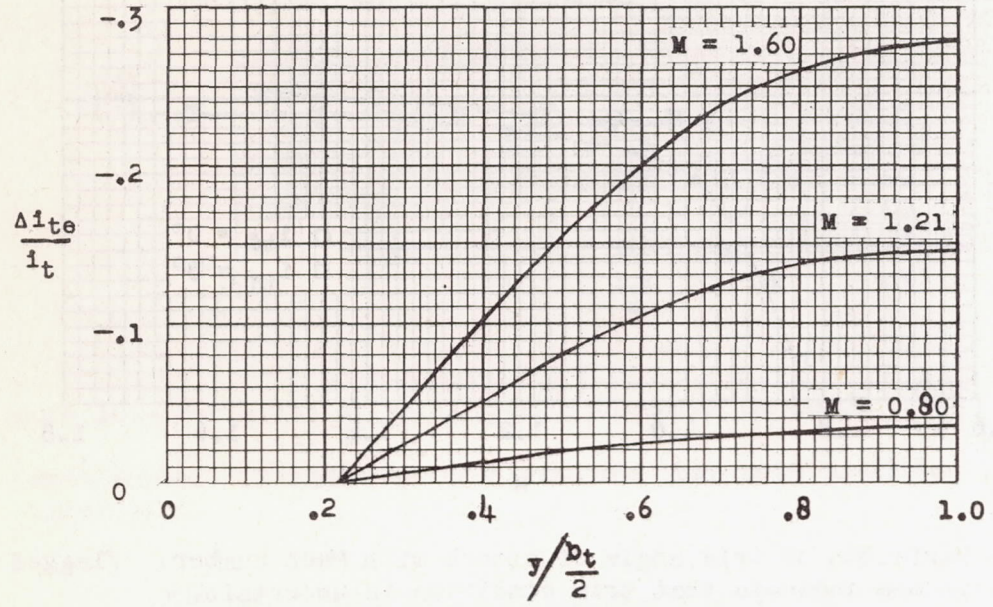
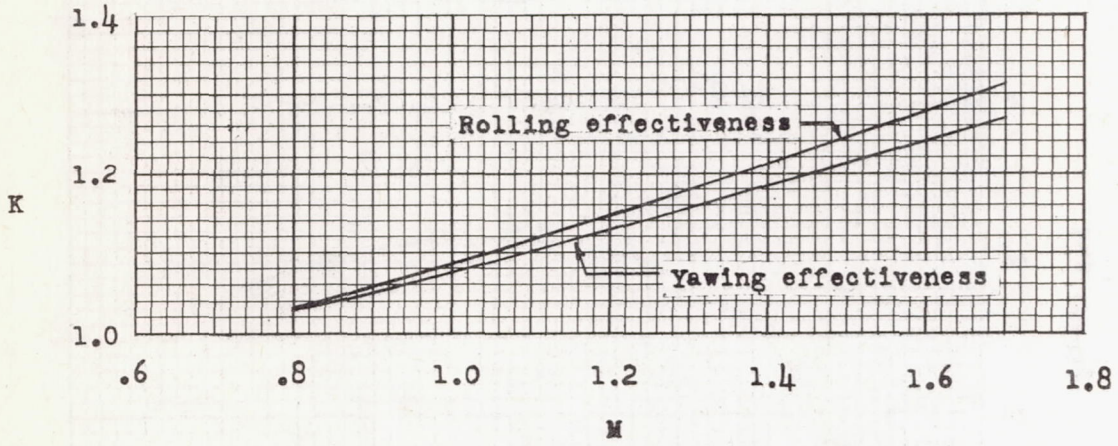


Figure 6.- Typical time history.



(a) Twist distribution.



(b) Aeroelastic correction factor.
Rigid effectiveness equals K × Measured effectiveness.

Figure 7.- Estimated aeroelastic properties of control surface.

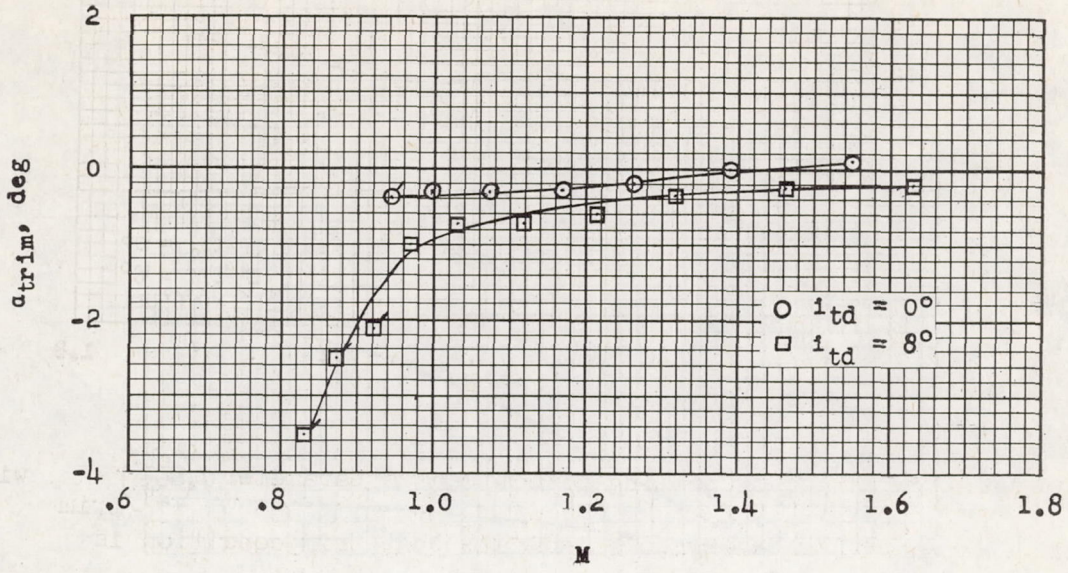


Figure 8.- Variation of trim angle of attack with Mach number. Flagged symbols indicate that trim condition is uncertain.

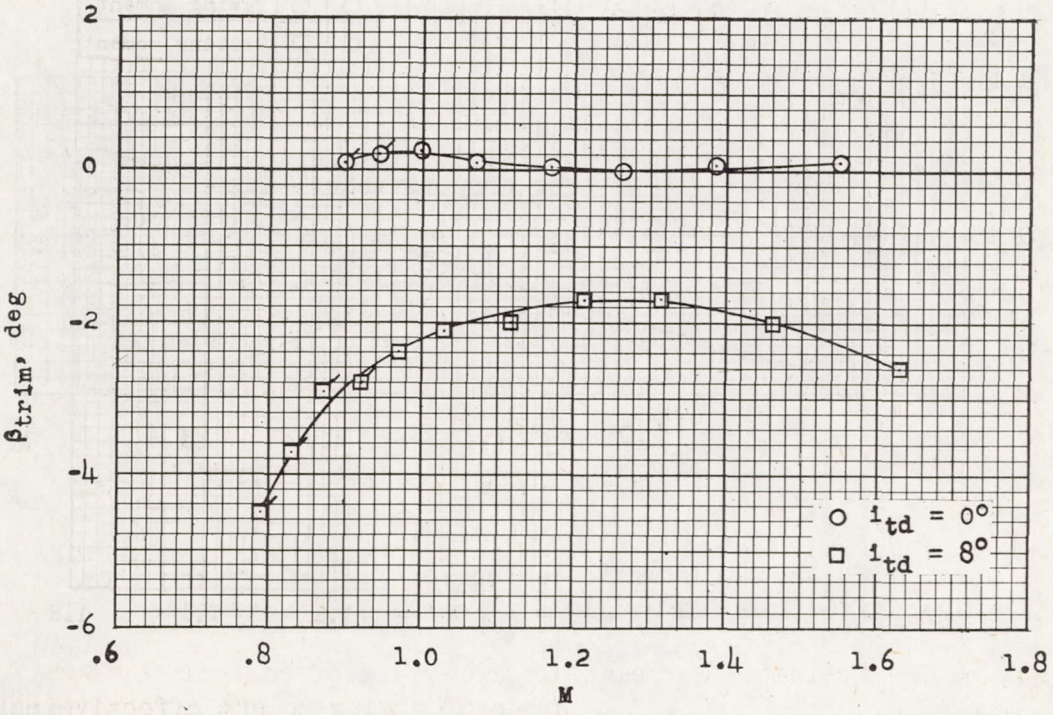


Figure 9.- Variation of trim angle of sideslip with Mach number. Flagged symbols indicate that trim condition is uncertain.

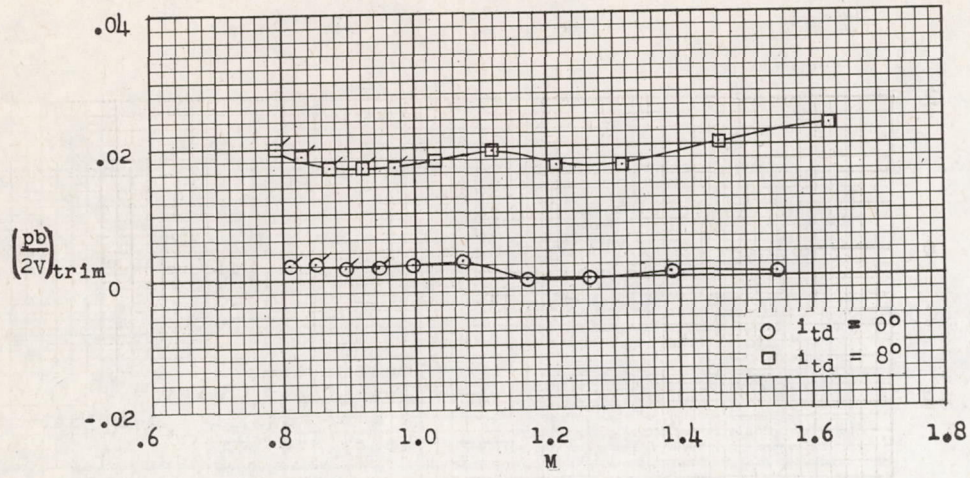


Figure 10.- Variation of rolling-effectiveness parameter $\left(\frac{pb}{2V}\right)_{trim}$ with Mach number. Flagged symbols indicate that trim condition is uncertain.

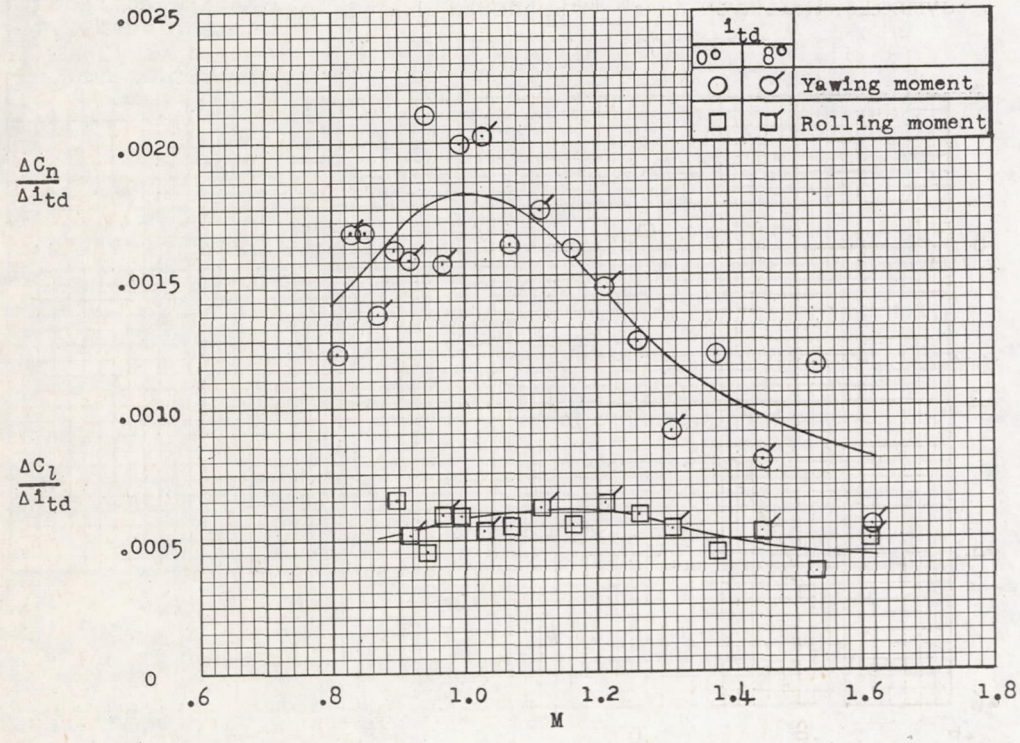


Figure 11.- Variation with Mach number of yawing-moment effectiveness $\frac{\Delta C_n}{\Delta i_{td}}$ and rolling effectiveness $\frac{\Delta C_l}{\Delta i_{td}}$ of differentially deflected tail surfaces.

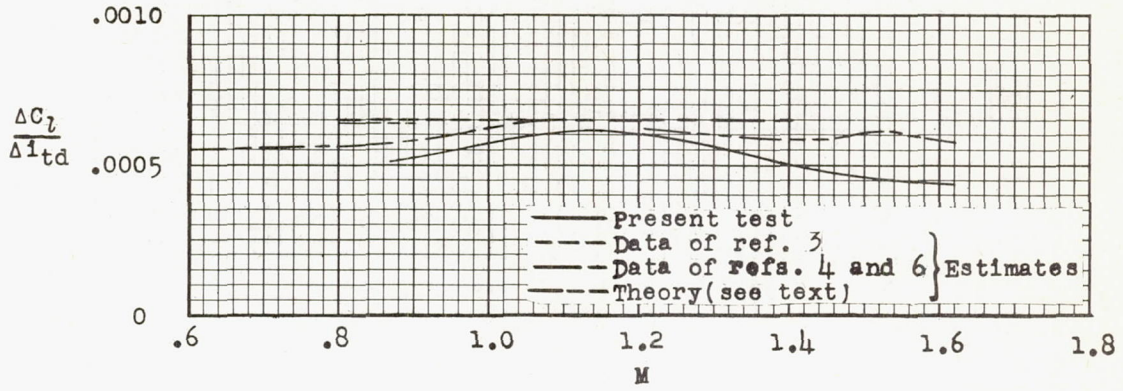


Figure 12.- Comparison of rolling-moment effectiveness with other results.

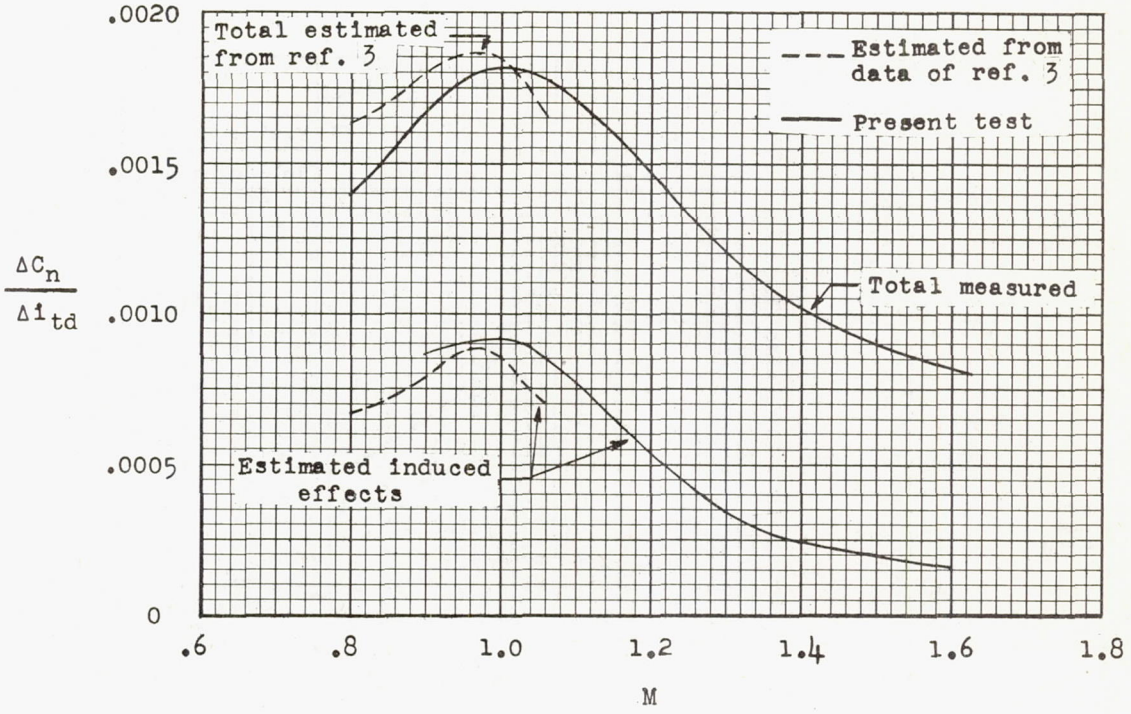


Figure 13.- Comparison of yawing-moment effectiveness with other results.

NACA - Langley Field, Va.

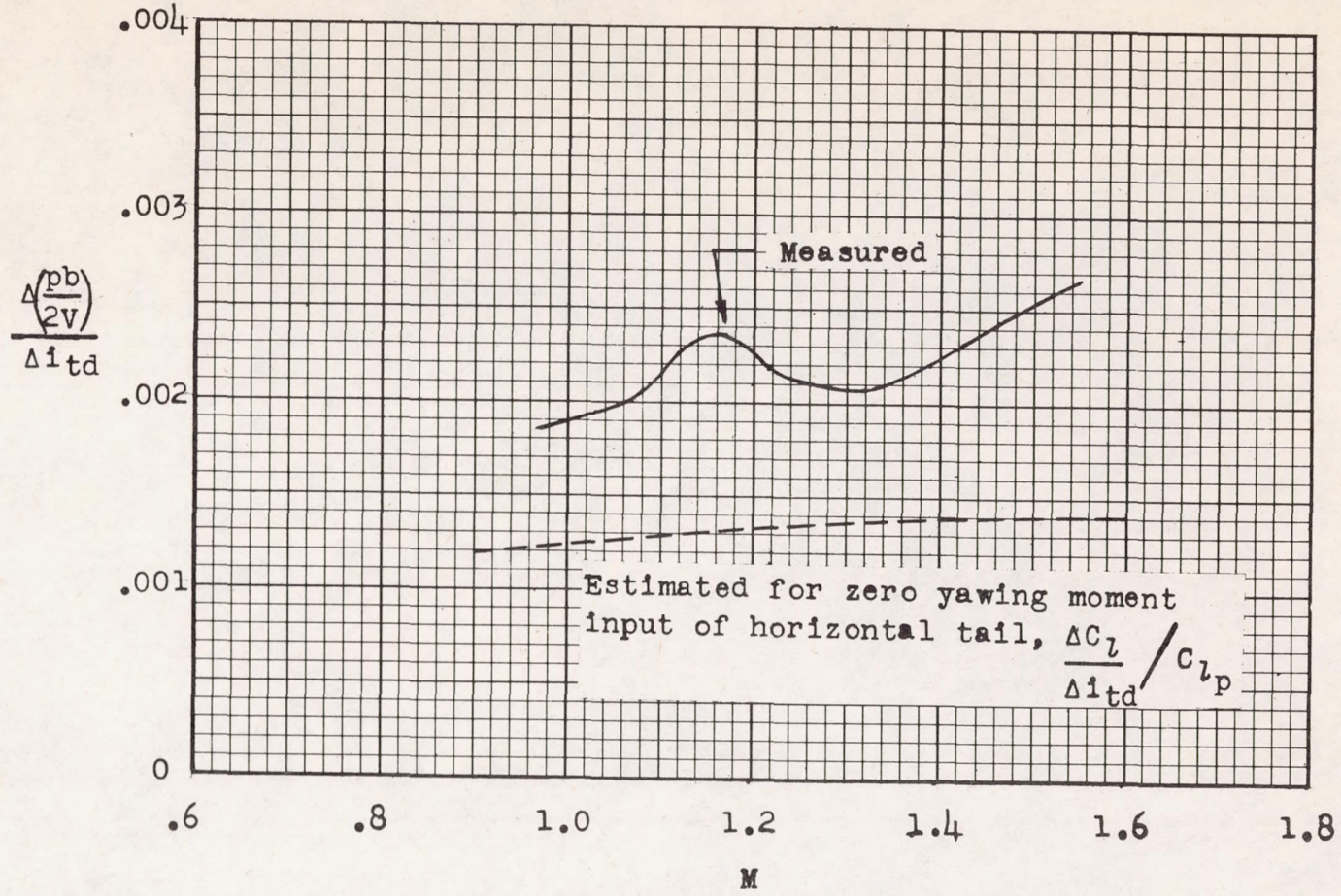


Figure 14.- Variation of rolling-effectiveness parameter $\Delta\frac{pb}{2V}/\Delta i_{td}$ with Mach number.